

# Pipeline internal coatings and aerodynamic testing of coatings

## Contents

### 1\_Introduction

### 2\_Pipe internal coatings

2.1\_Some types of internal coatings

2.2\_Coating surface characterisation

### 3\_Aerodynamic testing of coatings

3.1\_Description of the test apparatus

3.2\_Procedure for analysing the test results

3.3\_Aerodynamic test results

3.4\_Transposition of test results to an industrial case

### 4\_Conclusion

## 1\_Introduction

The prediction of pressure losses in a straight cylindrical conduct does not present major difficulties when knowing the flow conditions, the fluid properties and the internal wall roughness of a bared conduct. This requires the calculation of the friction factor which may be obtained from empirical equations adapted to the situation, particularly, the Reynolds number, the pipe diameter and the roughness (hydraulic roughness). These equations have been established following the testing of an extremely large range of flow conditions (gas types, pipe diameters, pressures and temperatures) and are therefore relatively reliable.

The prediction of pressure losses for a pipeline covering a long distance is more complex requiring the use of many correcting parameters: the effect of junction welds

(spiral welds for some pipelines), the change in pipe geometry (elevation, bends) and in operating conditions (pressure, temperature) with the distance and also the local occurrence of two phase flow, particularly at low points.

**The situation is relatively more complex for an internally coated pipe considering the specific characteristics of the coated surface and the effect of the coating material on gas transport.**

**A coating surface presents a complex geometry as it may include deformations of short, medium and large wave lengths** requiring the characterization of the profile with a roughness meter and for several cut off lengths. In addition, the importance of a particular wave length varies considerably with the coating type and the application method.

**The aerodynamic effect of the coating material** is even more complex as it varies with the coating type (its composition), the Reynolds number (or viscous layer thickness) and the pipeline operating conditions. As such, **the friction factor of a specific coating may vary considerably during its life from a newly applied coating to an aged coating as a result, for instance, of its contact with chemical agents.**

For these reasons, it is difficult to set a proper hydraulic roughness to calculate the friction factor. In some cases, the friction factor may be underestimated when disregarding the deformations with a medium or large wavelength (also called undulations). Considering the material effect, the situation may be even more complex, the friction factor being overestimated in the case of a new coating or underestimated in the case of an aged coating.

Prior to predict the fluid friction factor for internal coatings it is necessary to test them aerodynamically in their conditions of industrial applications considering the film thickness, the material type and the coating process at coater works. The friction factor corresponding to its industrial use is then transposed by applying a correcting law using Reynolds numbers and diameters (or the viscous layer) for both the test and the industrial conditions.

Testing a coating in conducts in industrial conditions may be extremely costly considering the condition of gas velocity and pressure (in fact, the product of these two parameters), the requirement for an extremely long loop to establish an equilibrium condition also the numerous associated equipment such as gas boosting units (compressors, heat exchangers, stabilizers, etc.) and metering devices (pressure, temperature, flow, gas analysis with redundancy for all of them).

To overcome this problem, **a very compact apparatus has been designed to test any type of cylindrical walls** (bared or coated steels or surfaces with flow reduction devices). This apparatus requires only a few litres of gas and may operate up to 100 bar with the gas circulating up to 40 m/s simulating all cases with the same conditions of product of pressure and gas velocity (for instance, 400 bar and 10 m/s). This apparatus does not require the need for compressors nor complex instrumentation.

## 2\_Pipeline internal coatings

### 2.1\_Some types of internal coatings

Several types of internal coatings from different sources (manufacturers) have been analysed regarding their surface profiles and their aerodynamic properties.

**Solvent based epoxy** coatings have been used extensively in the past but due to their high Volatile Organic Content (VOC) their use has been considerably restricted.

**Water based epoxy** coatings are intended to replace progressively the above ones due to their greater compatibility with the environment. These two types of coatings form a “dry film” after evaporation of the solvent.

**Powder epoxy** coatings do not contain any solvent. They are made of very small particles which are projected on the pipe internals brought to a very high temperature. Particles melt at their contact forming a film during the cooling process.

**Polyamide 11** coatings are thermoplastic polymers.

Before applying coatings, tube internals are sand blasted with large size particles (high roughness) to provide coating anchorage and to remove any trace of rust until white metal appears at the steel surface. They are then swept with high pressure air to remove any particles and dust before the coating process takes place.

Following coating application, the assembly of steel and coating is represented on figure 2.1 using a scanning beam microscope.

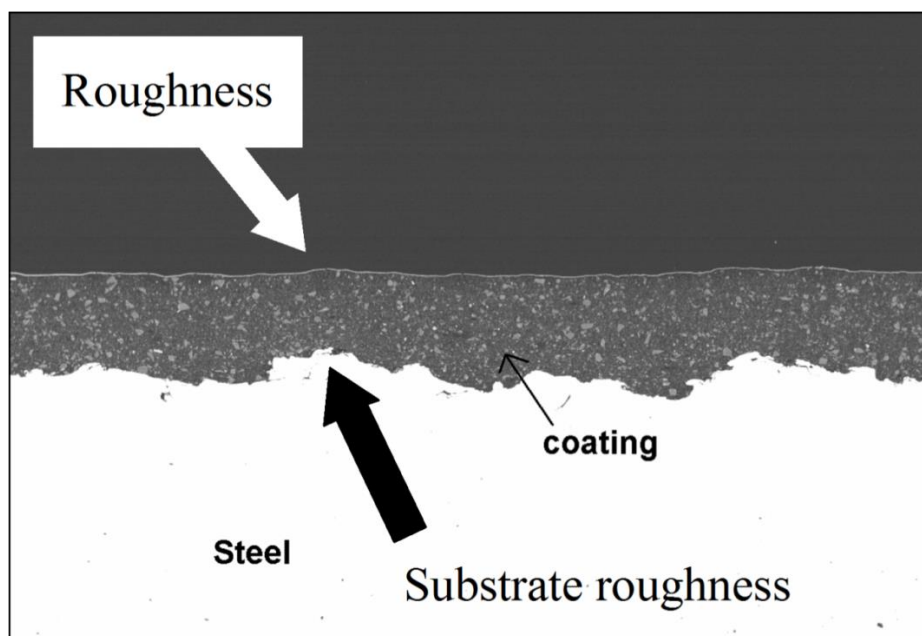


*Figure 2.1 – Scanning beam microscope - Cross section of a coating applied on a sandblasted steel surface. The dry film thickness is an average of 120 microns while the roughness of the steel surface is of the order of 70 microns (Rz).*

## 2.2\_Coating surface characterisation

ISO 4287 specifies terms, definitions and parameters for the determination of a surface texture (roughness, waviness and primary profile). The roughness value is obtained from the primary profile by filtering the longest wave components with several numerical approaches to finely characterize the surface.

Below are some parameters for characterising the surface roughness.

**Parameter  $R_z$**  represents the maximum height of the profile. It is the sum of the largest profile peak height,  $Z_p$  and the largest valley depth,  $Z_v$ , therefore:

$$R_z = Z_p + Z_v$$

**Parameter  $R_c$**  represents the mean value of the profile element heights,  $Z_t$  within the sampling length. The  $m$  element heights are measured from a local valley to the next local peak, therefore:

$$R_c = \frac{1}{m} \sum_{i=1}^m Z_{t_i}$$

**Parameter  $R_a$**  represents the arithmetical mean deviation of a roughness profile. It is the arithmetical mean of the absolute ordinate values  $Z(x)$  within the sampling length,  $L$ . The  $Z(x)$  values refer to the mean line over the sampling length, therefore:

$$R_a = \frac{1}{L} \int_{x=0}^{x=L} |Z(x)| dx$$

**Parameter  $R_q$**  represents the root mean square value of the ordinate values  $Z(x)$  within the sampling length,  $L$ . The  $Z(x)$  values refer to the mean line over the sampling length, therefore:

$$R_q = \sqrt{\frac{1}{L} \int_{x=0}^{x=L} Z^2(x) dx}$$

$R_a$  and  $R_z$  are the most currently used parameters. Previous measurements with profile meters have shown a relative constant ratio between the two parameters, with  $R_z / R_a \approx 5$ . However the numerical processing of profiles presenting relatively different shapes provides different ratios varying in an interval of 4 to 6. The value of the ratio depends on the statistical distribution of the elements. (Figure 2.2.1)

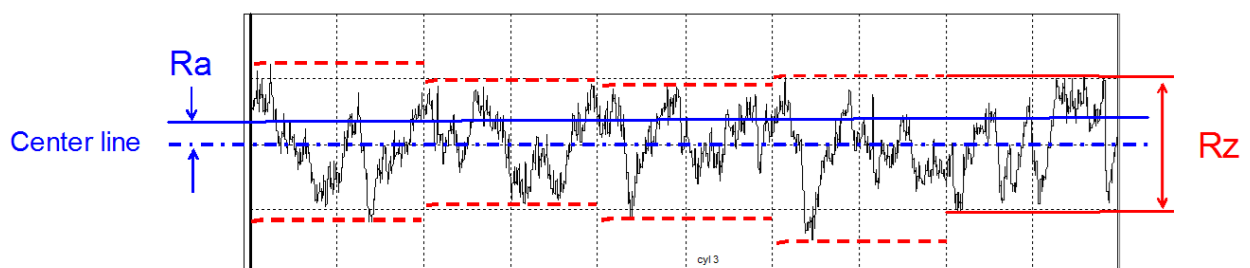


Figure 2.2.1 – Roughness measurements carried at a material surface with  $R_a$  and  $R_z$ .

Following profile analysis on coating and steel surfaces, it appears a major difference on the wave length of the profile change. The coating surfaces may present medium

height variations over small distances (roughness) together with larger height variations over large distances (undulations) contrary to steel surfaces which present only variations of the roughness type. Figure 2.2.2

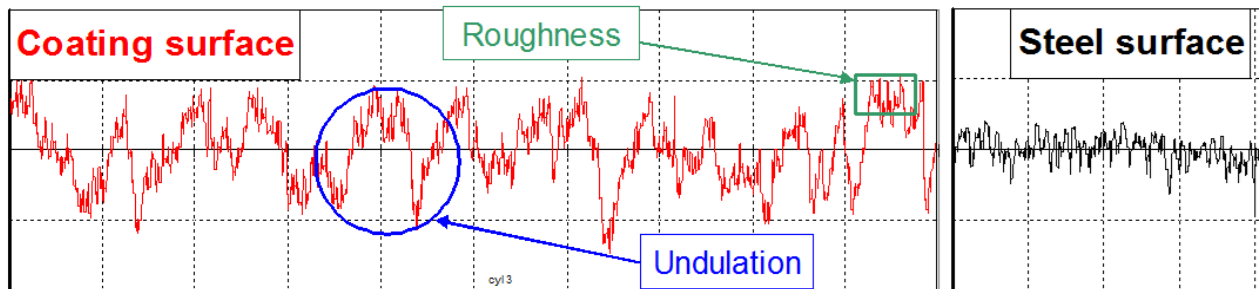


Figure 2.2.2 – Roughness profile with representation of roughness and undulation for coating and steel surfaces.

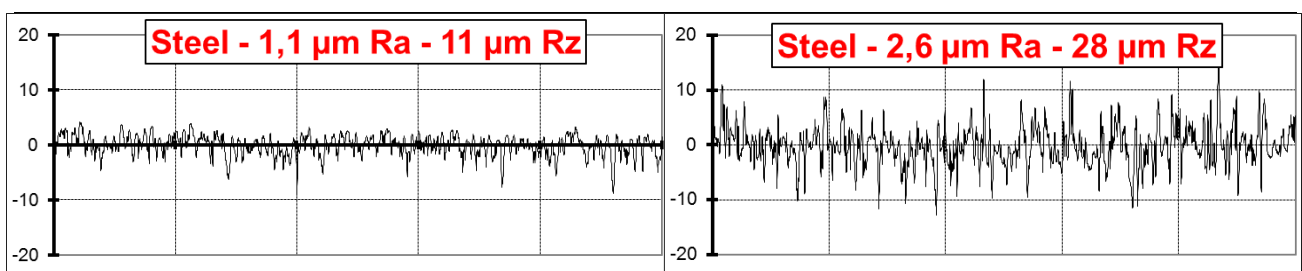


Figure 2.2.3 – Roughness profile for two steel surfaces with different roughness values.

Figures 2.2.4 illustrate the typical surface profile of several coating types. This could vary significantly with coater products and coating application. Nevertheless it provides general information on the specificity of the following coating types.

The solvent based coating presents a roughness height of a few microns with larger undulation amplitude of the order of 10 microns.

The water based coating presents a roughness height of a few microns with larger undulation amplitude of the order of 20 microns. The undulation amplitude is twice the above one. In some cases, these undulation amplitudes can reach 40 microns.

The solvent less coating hardly presents any roughness deformation while the undulation amplitude is an average of 5 microns.

The powder coating is relatively similar to the solvent less coatings with hardly any roughness deformation while the undulation amplitude is an average of 8 microns.

The polyamide 11 is relatively similar to the solvent less and the powder coatings with hardly any roughness deformation while the undulation amplitude spreads between 10 to 20 microns with considerably large wave length.

It appears from these profiles that to characterize a surface profile it is necessary to measure the Ra and Rz parameters with different cut off lengths, typically, 0.8 mm, 2.5 mm and 8.0 mm to get a more exact quantitative representation of these coating surfaces.

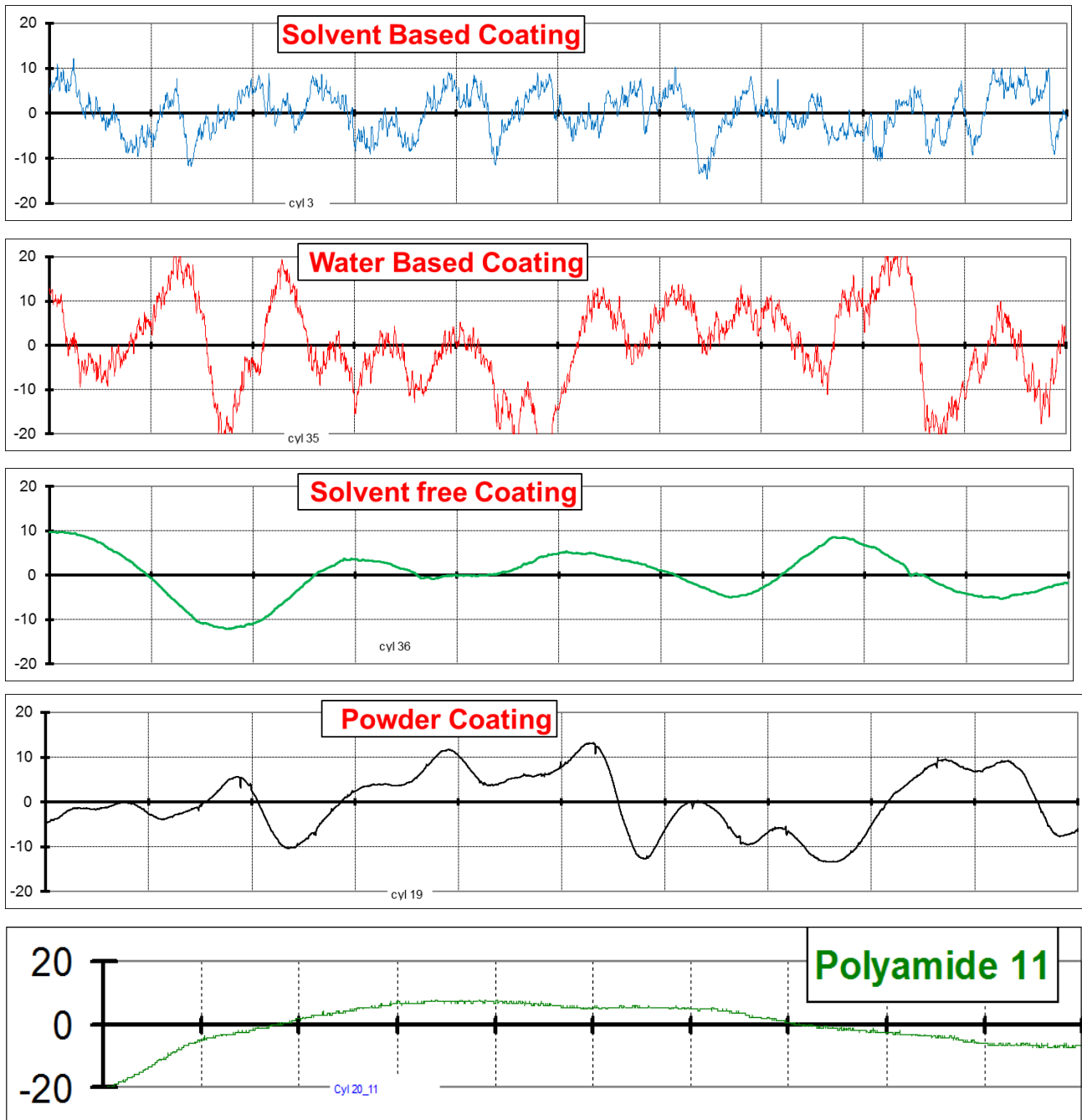


Figure 2.2.4 – Typical surface texture and profile for several internal coatings.

Another important parameter is the **dry film thickness** measured following full evaporation of the solvent. This effect is presented on figure 2.2.5 where it is seen that for a small film thickness (60 microns), the Rz roughness reaches 25 microns while for a relatively large film thickness (140 microns), the Rz roughness goes down to 10 microns with an intermediate roughness for an intermediate film thickness. These measurements were carried out at a cut off length of 2.5 mm.

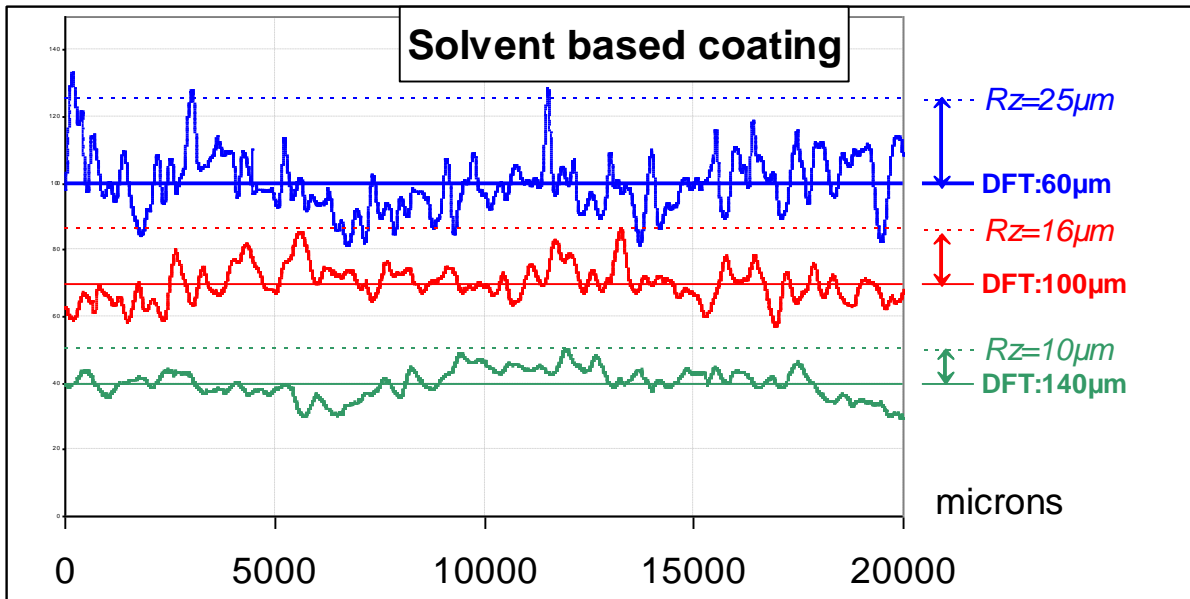


Figure 2.2.5 – Effect of the dry film thickness on the roughness at the surface of a solvent based coating. Roughness measurements made at a Cut Off of 2.5 mm.

For coatings, the selection of the cut off value is extremely important as it determines the degree of roughness and undulation of a specific profile. As an example, on figure 2.2.6, with a cut off of 0.8 mm, the largest undulations are filtered out providing a roughness amplitude of 10 microns Rz while with a cut off 10 times greater (8 mm) the undulation amplitude amount to 17 microns Rz. In between, a cut off of 2.5 mm provides an amplitude of 14 microns including only a fraction of the undulations (intermediate wave lengths). The measured points are plotted on figure 2.2.6 together with a representation (illustration) of the variation of Rz versus the dry film thickness.

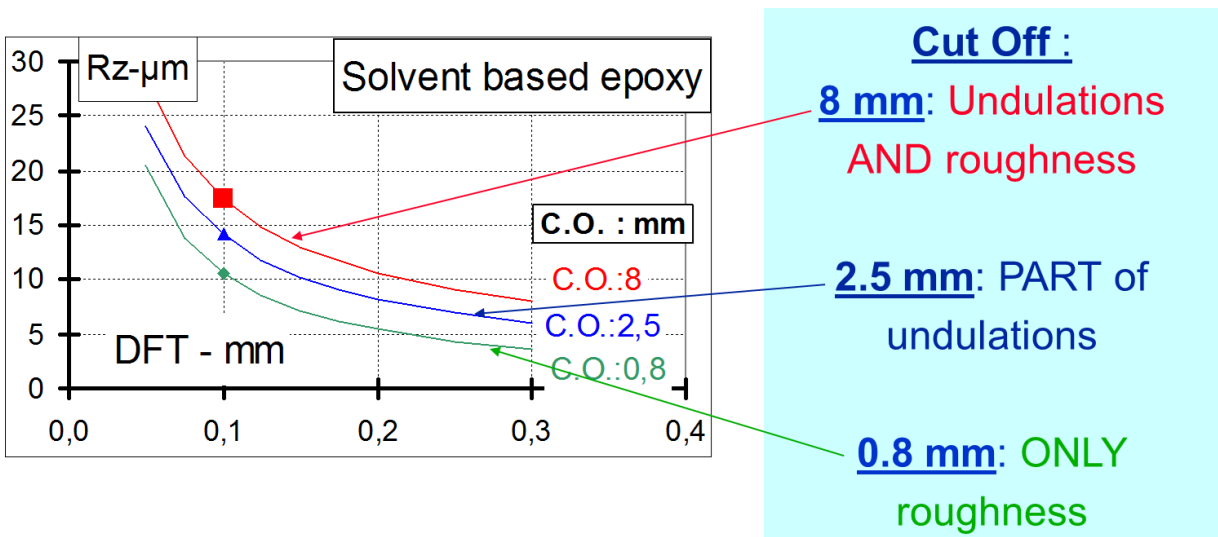


Figure 2.2.6 – Effect of the cut off length on the roughness amplitude – Solvent based epoxy.

In the case of the solvent based coating (figure 2.2.6), the ratio between measurements taken at 8.0 and 0.8 mm is relatively small, less than 2 showing a

significant but moderate importance of the undulations. However, in the case of water epoxy and solvent based epoxy, this ratio could approach 10 showing the extreme importance of the undulation in a profile analysis (figure 2.2.7). Disregarding, the undulation in a friction factor coefficient could lead to an underestimation of the pressure losses in a pipeline.

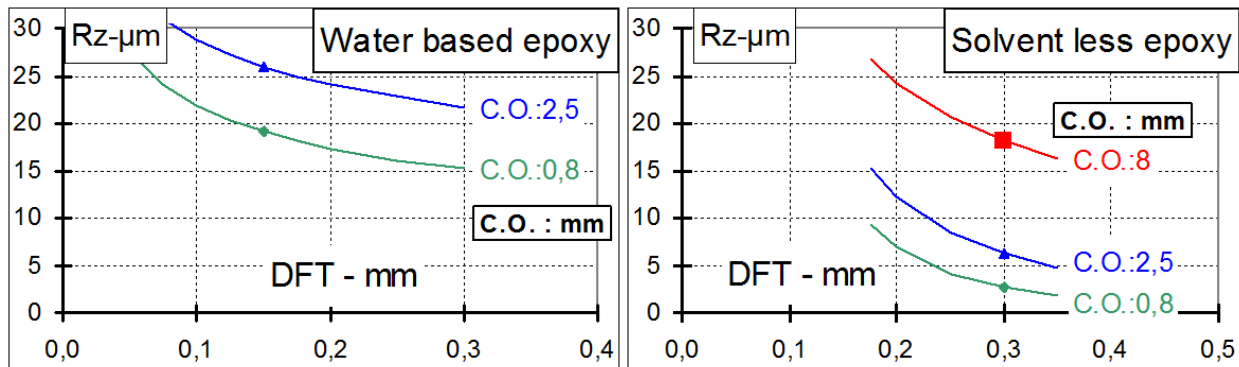


Figure 2.2.7 – Effect of the cut off length on the roughness amplitude – Water based and solvent less epoxies.

### 3\_Aerodynamic testing of internal coatings

#### 3.1\_Description of the test apparatus

The test apparatus appears externally as a cylindrical vessel designed for an operating pressure of 100 bar (figure 3.1.1). When it is installed vertically on its support it presents a bolted flange at a top end to provide an access to the cylinder internals and an electric motor at the bottom end for driving an internal cylindrical rotor.

The test apparatus operates on the following principle:

- A Cylindrical tube is inserted inside the high pressure vessel surrounding a rotating cylinder moved by an underneath electric motor.
- After closing of the vessel with the upper flange, the vessel is pressurised with a pure gas, for instance, argon or nitrogen (Figure 3.1.2 – Left)
- The rotation of the internal cylinder causes the entrainment of the high pressure gas which, in turn, is slowed down by the internal surface of the fixed cylindrical tube.
- A Pitot tube mounted at mid distance between the fixed tube and the rotating cylinder measures the intermediate gas velocity (Figure 3.1.2 – Right). This velocity is dependent on the roughness of the internal surface of the external tube. Alternatively, a torque meter mounted in between the electric motor and the internal cylinder could measure the resisting torque caused by the high pressure gas and the roughness of the external tube.

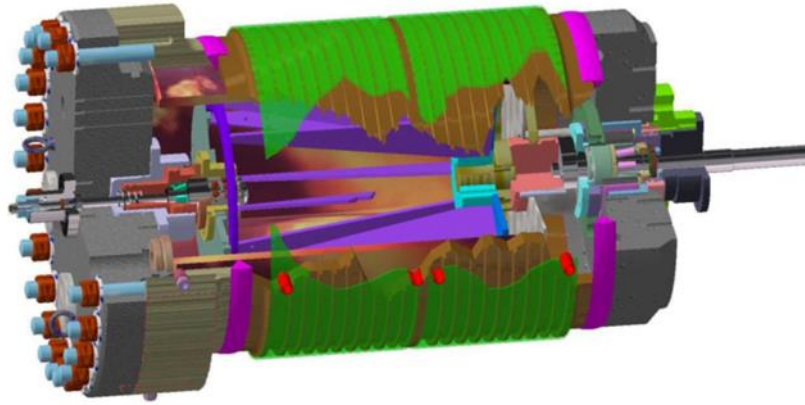


Figure 3.1.1 – Rotating Cylinder Unit (RCU) for aerodynamic testing of the internal surface of an external cylindrical tube.

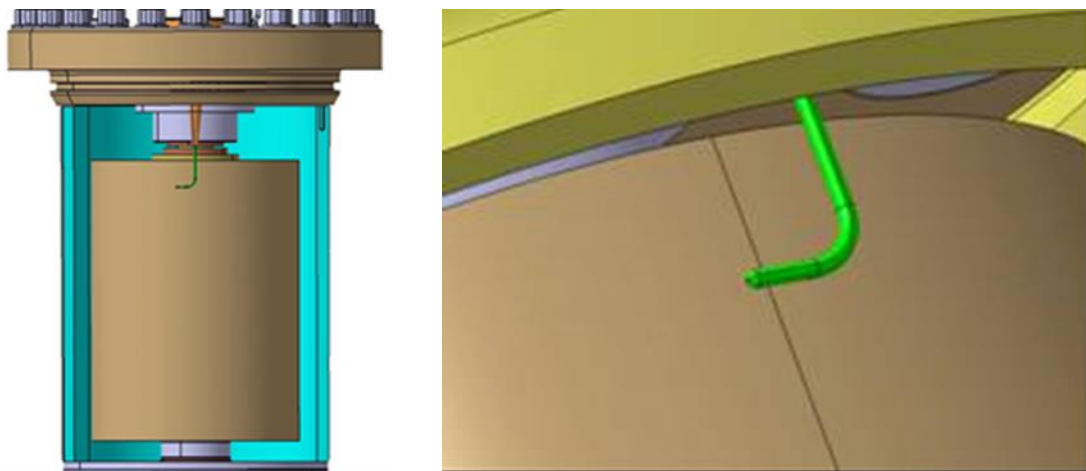


Figure 3.1.2 – Left: Cross section of the Rotating Cylinder Unit (RCU) for aerodynamic testing of a cylindrical wall surface. Right: Pitot tube for gas velocity measurement.

The gas velocity in between the two cylindrical surfaces is dependent on: a) the peripheral velocity of the internal rotating cylinder; b) the radial distance between the two walls; c) the roughness of the internal surface of the fixed tube which is the piece of equipment which needs to be evaluated and d) the gas properties.

The gas velocity variation versus the distance to the centre of rotation and the wall roughness of the fixed tube is shown on figure 3.1.3. It has to be noted that the Pitot tube being mounted in a fixed position, it measures only a single value for a given wall roughness. The velocity profiles shown on figure 3.1.3 were determined by flow simulation with a CFD code as it cannot be established with the Pitot tube mounted at a fixed position.

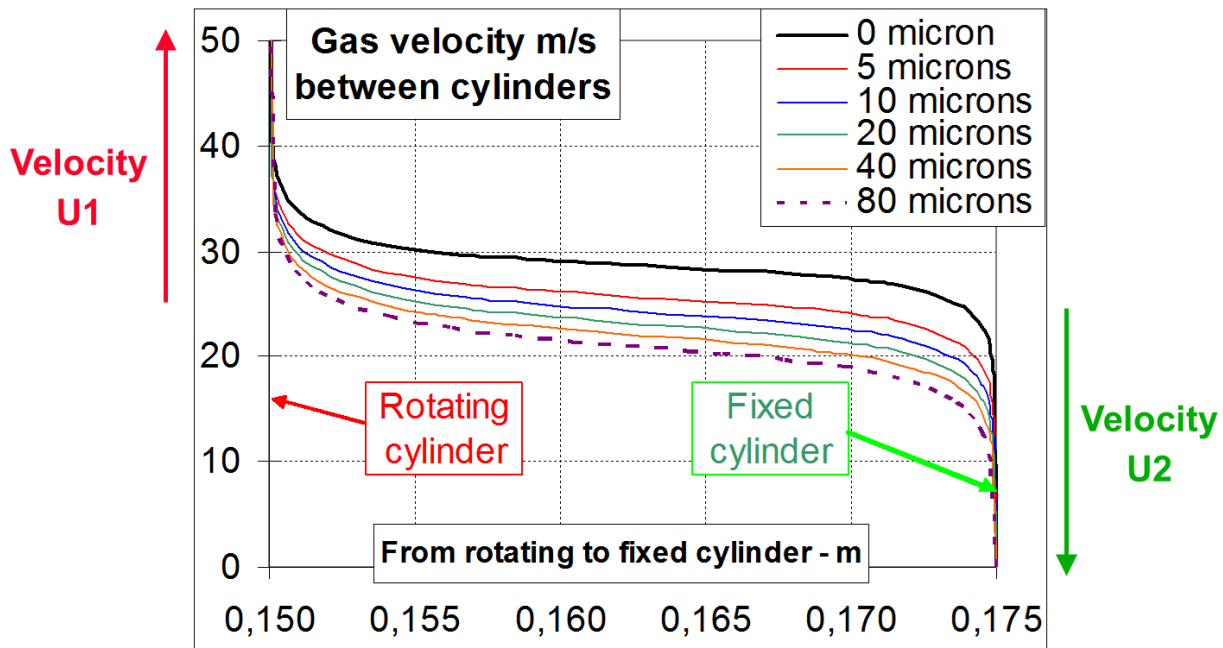


Figure 3.1.3 – Gas velocity profiles (versus distance to the axis of rotation) between the external fixed tube and the rotating cylinder for several wall roughness of the fixed wall. Inner cylinder rotating at 4000 rpm.

A gas velocity curve is made of six segments.

The first set of the three segments at the fixed tube side includes: a) a **laminar layer** represented by a straight line with extremely small slope, extending at a very small distance to the wall but with a considerable velocity decrease (gas slowed down by the fixed wall); b) a **sub turbulent layer** represented by a slightly curved line and extending also at a very small distance to the wall; c) the **turbulent core** applying from the core centre to the end of the sub layer. In that core, the velocity is relatively constant, increasing very slightly from the end of the sub layer to the central core. The velocity profile presents a curved shape with the concavity oriented towards the laminar layer (zero velocity line).

The second set of the three segments at the rotating cylinder side is symmetrical to the first one: It includes also: a) a **laminar layer** with a considerable velocity increase relative to the wall (gas entrainment). Referring to the peripheral velocity it is a velocity decrease; b) a **sub turbulent layer** with another velocity reduction; c) the **turbulent core**. In that layer, the velocity is relatively constant, decreasing very slightly from the end of the sub layer to the central core. The velocity profile presents a curved shape with the concavity oriented towards the laminar layer (peripheral velocity line).

The two turbulent regimes (one for the fixed wall and one for the rotating wall) join in the middle of the central core. **The velocity magnitude at the joining point is dependent on the roughness of the fixed wall. This is also the value measured by the Pitot tube.**

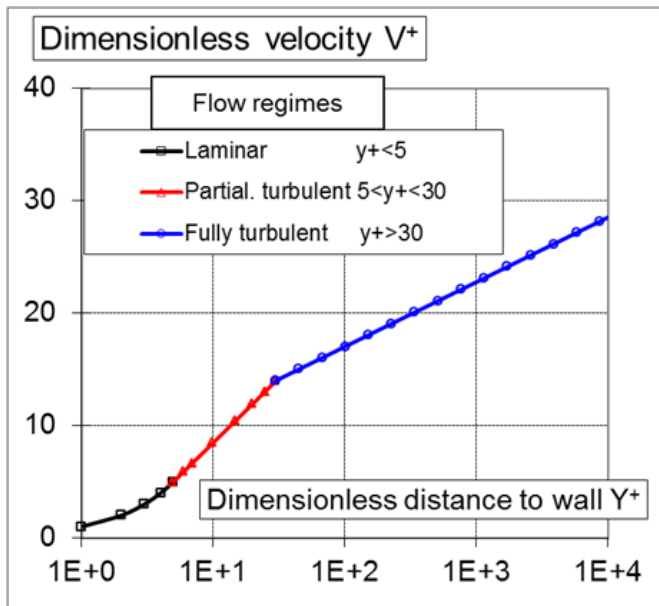


Figure 3.1.4

Representation of the three segments (flow regimes) from the wall to the central core: laminar, sub layer (partially turbulent) and central core (fully turbulent).

Graph plotted with dimensionless velocity versus dimensionless distance to the wall.

To note the logarithmic scale of the abscissa.

There is a main difference in gas displacement between the test apparatus case and a conduct case. In the test apparatus case, the gas moves with a circular motion (in the radial plane, perpendicular to the axis of the tube). In the conduct case, the gas moves longitudinally (in a transversal plane passing through the tube axis). It is assumed that there is no incidence on the measurement of the hydraulic roughness as all the coating processes (from tube sand blasting to coating spraying) leads to an isotropic deposition of the coating film.

### 3.2\_Procedure for analysing the test results

The dimensionless parameter  $U1/U2$  (figures 3.1.3 and 3.2.1) is used to determine the hydraulic performance of the internal surface of the fixed wall where  $U1$  is the velocity relative to the fixed wall and  $U2$  is the velocity relative to the rotating wall.

$U1$  is the velocity measured by the Pitot tube while  $U2$  is the difference between the peripheral velocity of the rotating cylinder  $U_p$  and  $U1$ .

Plotting the parameter  $U1/U2$  versus the roughness of the fixed wall one obtains figure 3.2.1. As it is shown by the results of the CFD calculation presented on figure 3.1.3, the parameter  $U1/U2$  increases with the wall roughness. The  $U1/U2$  was established experimentally by using several steel cylinders with different roughness values (calibration phase). The steel cylinders were blasted with sand particles of different size (granulometry). The parameter  $U1/U2$  is plotted for a given Reynolds number where the equivalent hydraulic diameter is the distance between the fixed and rotating walls and the gas velocity is half the peripheral velocity of the rotating wall. In the present case the Reynolds number is  $9E6$ .

**$U1/U2$  is called the friction parameter.**

To establish the hydraulic roughness of a tested wall, it is:

- First necessary to calculate the Reynolds number corresponding to the operating conditions (pressure, temperature, gas type) providing the viscosity and volumetric mass of the gas,
- In second, to calculate the friction parameter  $U1/U2$  from the Pitot tube measurement,
- In third, the friction parameter is plotted versus the physical roughness of the wall.

The results are then interpreted by plotting a horizontal line crossing the “steel” line. At the junction of the steel line, plotting a vertical line provides the hydraulic roughness of the fixed wall. In the case of the coatings represented on figure 3.2.1:

- The red square symbol, the hydraulic roughness is 1 micron while the physical roughness is 3 microns Ra.
- The green triangle symbol, the hydraulic roughness is 0.5 micron while the physical roughness is 2 microns Ra.
- The blue diamond symbol, the hydraulic roughness is 0.4 micron while the physical roughness is 1.2 micron Ra.

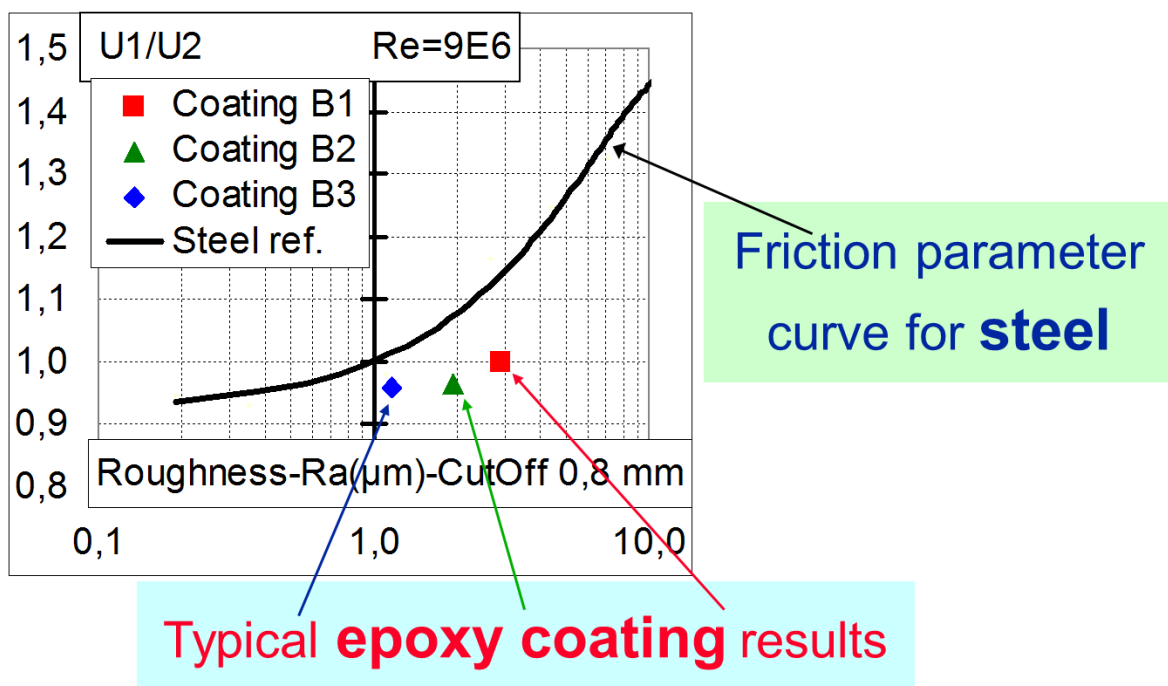


Figure 3.2.1 – Friction parameter  $U1/U2$  versus the physical roughness for a given Reynolds number - Sand blasted steel (reference line) and three epoxy coatings.

### 3.3\_Aerodynamic test results

The results of an aerodynamic test may be presented for different Reynolds number values which may be obtained by varying either the running speed of the rotating cylinder or the pressure inside the test apparatus.

Comparing figure 3.2.1 and figure 3.3.1 (left) one can see the effect of the Reynolds number. By reducing it from 9E6 to 3E6, there is a smaller sensitivity, in the second case, of the coating profiles due to a larger viscous layer thickness when the Reynolds number is smaller.

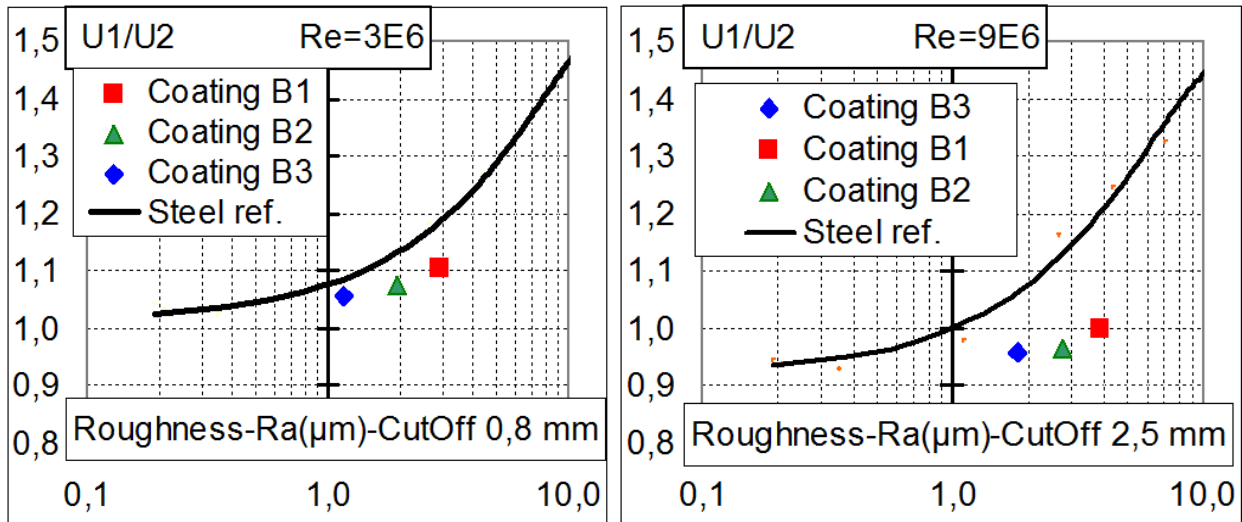


Figure 3.3.1 – Friction parameter  $U1/U2$  versus the physical roughness  $Ra$  - Left: Reynolds number  $3E6$  and cut off  $0.8mm$ . Right: Reynolds number  $9E6$  and cut off  $2.5mm$ .

Comparing figure 3.2.1 and figure 3.3.1 (right) one can see the effect of the cut off length (from 0.8 mm to 2.5mm) when estimating the hydraulic roughness from the physical roughness. If the cut off would have been taken greater (8.0mm), in the case of water based or solvent less coatings, the distance of the coating points to the “Steel” line would have been considerably greater (figure 2.2.7).

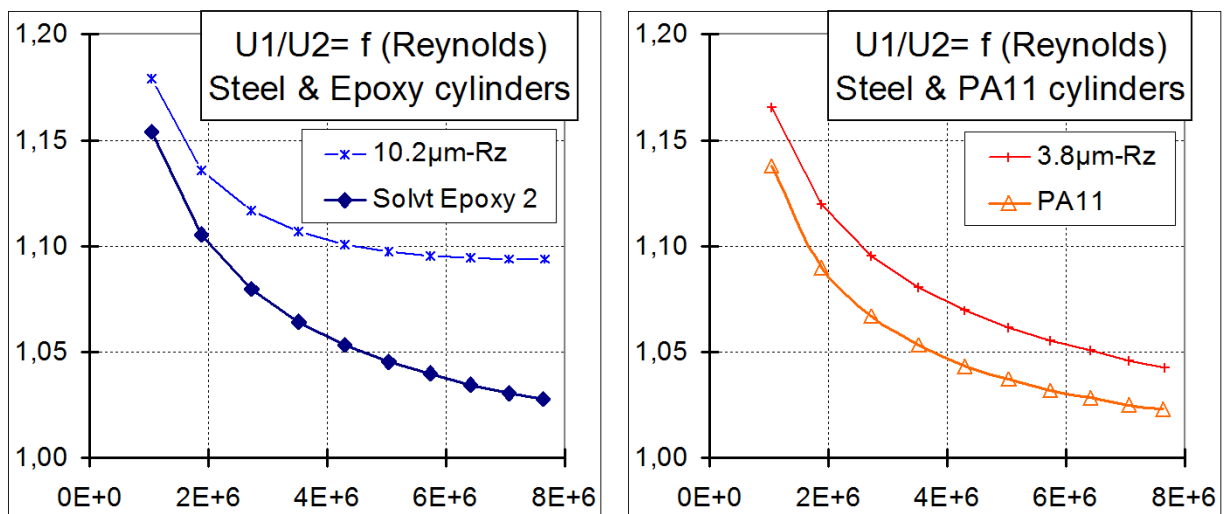


Figure 3.3.2 – Friction parameter  $U1/U2$  versus the Reynolds number. Left: an epoxy coating; Right: a polyamide coating.

Results are presented on figure 3.3.2 for two coating types, a solvent based coating (left) and a polyamide coating (right). In both cases, the performance of a coating

type is compared to the performance of a steel tube with the same roughness. To be exact, the solvent based coating presents a 10.0 micron roughness versus 10.2 microns for the steel surface and the polyamide coating presents a 3.0 micron roughness versus 3.8 microns for the steel surface.

It can be seen that in the two coating cases, **there is a material effect tending to reduce the hydraulic roughness**. This could be interpreted as a sliding effect at the coating surface. This could be the result of a repulsion of the gas molecules from the coating surface causing less interaction between the molecules and the wall and, consequently, less fluid friction.

On figure 3.3.2, the equivalent hydraulic roughness could be determined from several calibrated steel cylinders covering a large range of roughness values with, very often, a specific value for each Reynolds number.

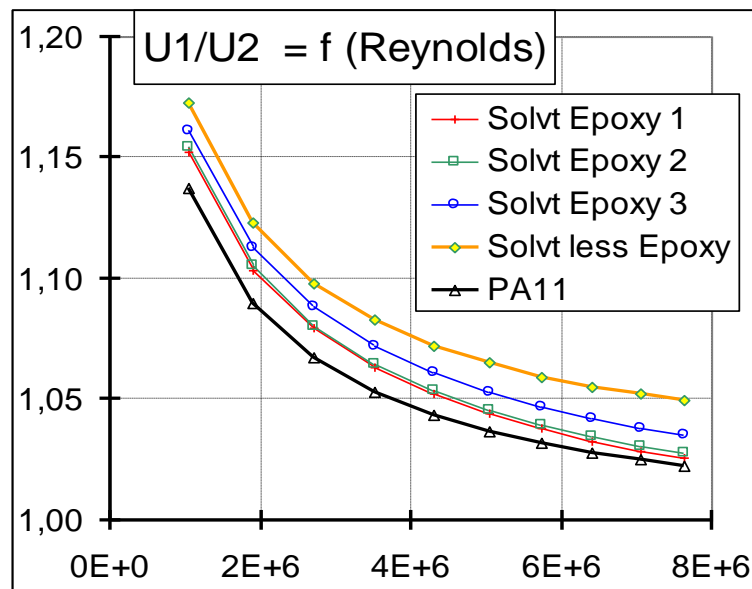


Figure 3.3.3 – Friction factor  $U1/U2$  for several coatings following testing. These results may vary slightly from one coating application to the other.

The friction parameter is plotted on figure 3.3.3 for three solvent based coatings, one solvent free coating and a polyamide coating. In the present situation, the solvent free coating provides the largest friction parameter probably due to the large amplitude of the undulations even its surface is absolutely smooth locally. To the contrary, the polyamide coating provides the smallest friction parameter probably due to undulations with extremely long wavelength not causing major vortices between undulation crests. The three solvent based coatings provide an intermediate friction parameter with larger roughness values but smaller undulation amplitudes. It is possible that the coating material amplifies some of these trends.

The impact of a change in hydraulic roughness on the friction factor (this is not the friction parameter) is presented on figure 3.3.4 taking a smooth surface as a reference. As an example, an increase in roughness from 0 to 10 microns causes an

increase in friction factor of 11% for a Reynolds number of 1E7. This increase is larger, 35 % for a Re number of 9E7.

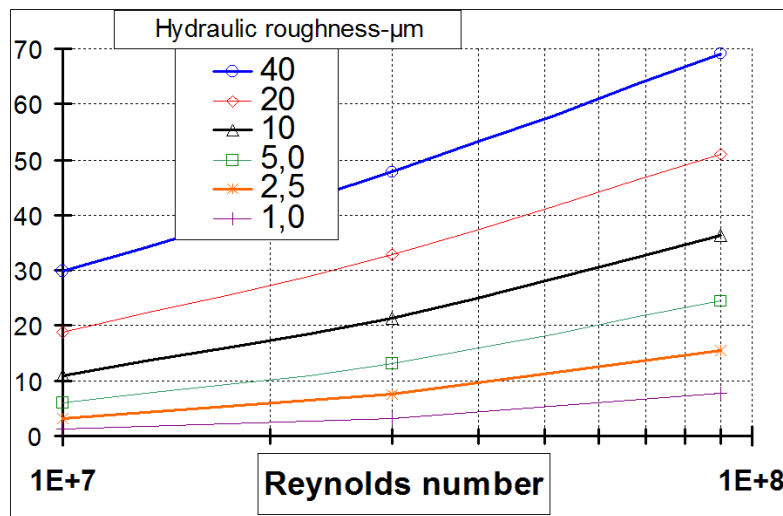


Figure 3.3.4 – **Friction factor increase** versus the roughness number and the Reynolds number. Reference: smooth surface

The figures are relatively smaller if one considers the reduction in friction factor based on a reduction in hydraulic roughness (figure 3.3.5). This may be the case when considering a steel surface as a reference and the benefit of a coating.

Re:	1E+7	3E+7	9E+7
40 to 0 μm	23	32	41
10 to 0 μm	10	18	27

Figure 3.3.5 – **Friction factor decrease** from 40 to 0 micron and 10 to 0 microns for several Reynolds number.

### 3.4\_Transposition of test results to an industrial case

Results may be transposed from one situation to another when they are linked by a condition of similitude.

Let's assume that the two situations are linked by the two following equalities:

- Same hydraulic roughness  $R_{h1}=R_{h2}$
- Same viscous layer thickness  $e_{vis1}=e_{vis2}$

The viscous layer thickness may be calculated from the flow conditions by:

$$e_{vis} = 5 \frac{D}{Re} \sqrt{\frac{8}{F_f}} = 5 \frac{\mu}{V\rho} \sqrt{\frac{8}{F_f}} \quad \text{with} \quad Re = \frac{VD\rho}{\mu}$$

The relation between the two friction factors is then:

$$\frac{1}{\sqrt{F_{f2}}} - \frac{1}{\sqrt{F_{f1}}} = 2 \log \frac{D_2}{D_1}$$

## 4\_Conclusion

**The characterisation of the surface profile of various coating types has shown the large spectrum of amplitude and wave length deformation.** The solvent based coatings present roughness amplitude smaller than steel but some deformations of a longer wave length. Water based coatings have shown significant roughness amplitude with relatively large undulation amplitude. To the contrary powder coatings present little roughness with some residual undulation amplitude. Like powder coating, polyamide coating has shown an extremely small roughness with undulation of a very large wavelength not detrimental to the aerodynamic performance.

A **test apparatus** has been developed for carrying aerodynamic test of internal coatings. It is suitable to an operation up to a gas velocity of 40 m/s and a pressure of 100 bar. Results found in these conditions may be transposed to any condition with a constant velocity \* pressure product (i.e. 20 m/s and 200 bar or 10 m/s and 400 bar).

All new coatings have presented a beneficial **material effect** tending to reduce the fluid friction compared to a steel surface based on the same surface roughness. This may be explained by a certain degree of repulsion of the gas molecules from the wall providing less contact between these two and therefore less fluid friction.

Following the aerodynamic testing of a coating in the rotating cylinder unit, it is possible **to transpose the friction factor** established during testing to any industrial applications following a transposition law based on an equality of the hydraulic roughness and viscous layer thickness values.

Aerodynamic performance of **aged coatings** will be reported in the Web Site Page "Pipelines" section "Aged coatings".